

# Atomic force microscopy imaging of hair: correlations between surface potential and wetting at the nanometer scale

Vincent Dupres,<sup>a</sup> Terri Camesano,<sup>b</sup> Dominique Langevin,<sup>a,\*</sup> Antonio Checco,<sup>c</sup> and Patrick Guenoun<sup>c</sup>

<sup>a</sup> *Laboratoire de Physique des Solides, Université Paris Sud, Orsay, France*

<sup>b</sup> *Department of Chemical Engineering, Worcester Polytechnic Institute, Worcester, MA, USA*

<sup>c</sup> *Service de Physique de l'Etat Condensé, CEA-Saclay, Gif sur Yvette, France*

Received 25 April 2003; accepted 13 August 2003

## Abstract

We report investigations of hair surface potential under wetting at the nanometric scale by atomic force microscopy (AFM). Surface potential imaging was used to characterize the electrostatic properties of the hair samples. We found that the surface potential noticeably increases along the edges of the cuticles. These results are correlated with wetting behavior of different liquids performed using AFM in noncontact mode.

© 2003 Elsevier Inc. All rights reserved.

*Keywords:* Hair surface; Atomic force microscopy; Surface potential; Wetting

## 1. Introduction

Hair is a natural fiber of typical diameter 70  $\mu\text{m}$ , with an extremely complex structure [1]. The hair surface is covered by a layer of intercalated flattened cells, called cuticles, resembling the scales of a snake's skin. The flat region of the cells is covered by a compact hydrophobic layer, mostly composed of fatty acids; the side of the cells is less hydrophobic, and is covered in part by proteins.

In recent years, the structure of human hair has been widely studied by numerous techniques. Among them are optical microscopy, scanning electron microscopy (SEM), transmission electron microscopy (TEM) [2–6], and X-ray microdiffraction [7]. Recently, the growing development of atomic force microscopy (AFM) has facilitated local investigations of hair structure [8–11], especially by providing more details of the cuticular surfaces [12]. This nondestructive technique appears to be a useful tool for the study of the surfaces of capillary fibers.

However, the local wetting properties of hair, and more generally of fibers, have received relatively little attention. Some experiments have been performed to determine the

contact angle between a fiber and different liquids, but these measurements remain macroscopic [13–17]. Moreover, it appears difficult to correlate the results with the microscopic structure of the sample. The local wetting properties are expected to be related to the local polarity, another property scarcely investigated. A special difficulty comes from the fact that the surface is porous to some liquids: in particular, hair swells considerably in the presence of water [18].

In this paper, we present an investigation of local wetting properties and polarity of human hair by atomic force microscopy. Surface potential imaging was used to map the local polarity of hair samples. The wetting properties of the samples were investigated using AFM in noncontact mode and using different liquids directly deposited on the hair surface.

## 2. Experimental

European brown virgin hair samples were used without any chemical treatment. Nevertheless, they were washed with a surfactant solution (20% sodium lauryl ethoxylated sulfonate) then subsequently rinsed thoroughly with distilled water before use in order to reduce the number of deposits which can be currently found on the cuticles. In this study,

\* Corresponding author.

*E-mail address:* [langevin@lps.u-psud.fr](mailto:langevin@lps.u-psud.fr) (D. Langevin).

we limited ourselves to the cleanest hair sections located near the root.

Two different atomic force microscopes were used during these studies. Surface potential experiments were performed on a Nanoscope III multimode AFM (Digital Instruments), connected to an extender electronics module, with electric force microscopy cantilevers (silicon with a conductive coating). The substrates were commercially available 12-mm-diameter doped silicon wafers (in order to be conductive) (Veeco Instruments). The wetting experiments were performed on a Park M5 AFM (TM microscope, Veeco Instruments) using the noncontact mode with silicon tips. This microscope possesses a large and movable platform which is very convenient for wetting investigations on bulky substrates; it increases the investigated area and allows us to use larger samples. The substrates used during these wetting experiments are hydrophilic silicon wafers or glass coverslips. During surface potential experiments, the hair was glued to a silicon chip using silver paint in order to ensure good electrical contact with the scanner. During the wetting investigations, either silver glue or two pieces of transparent tape were used to fix the hair sample to the substrate.

The liquids used to characterize the wetting properties of the hair were pure Millipore water, alkane (decane, dodecane) from Sigma (99% purity), glycerol (99% purity), silicone oil (PDMS, polydimethylsiloxane of viscosity 100 cS from Rhodia), and squalane (2,6,10,15,19,23-hexamethyl-tetracosane,  $C_{30}H_{62}$ ), a nonpolar branched hydrocarbon (Merck, > 99% purity).

Temperature and humidity were controlled during each experiment. Temperatures were in the range 20–24 °C ( $\pm 1^\circ$ ), while the relative humidity was 40% ( $\pm 5\%$ ).

### 3. Results

#### 3.1. Surface potential experiments

Two techniques are available to characterize electrical properties of samples using a Nanoscope III AFM connected to an extender electronics module: electric force microscopy (EFM) and surface potential imaging (SPI). Surface potential imaging was selected for this study; this technique is sometimes referred to as Kelvin probe force microscopy (KFM) [19,20]. It maps the local variations of the surface potential of the sample.

This technique is based on a two-pass lift-mode measurement across each line of scan. Topographical data are taken in tapping mode in the first pass. Then the tip is raised to a fixed height for a second scan (a constant separation is maintained between the tip and the surface using data obtained during the first scan); the mechanical oscillation occurring in tapping mode is then idle and an adjustable voltage is applied directly to the tip. During the travel of the tip above the hair sample, a difference of potential exists between the tip and the surface, which leads to the appearance of a force.

To compensate for this force, the voltage of the tip has to be adjusted so that the tip is at the same potential as the hair surface [19,20]. The voltage applied to the tip is then used to map the surface potential image. As a result, two images are captured successively for each sample: a topographic image and either an electric field gradient image or a surface potential image. Unless otherwise specified, an electric potential of 5 V was applied to the tip during all experiments.

Figure 1 shows a topographic image (a) and the corresponding surface potential image (b) of the same hair region. Similar images are observed for all the samples investigated. Despite the fact that all the hair samples were taken near the root end to obtain undamaged scale edges, several of the images indeed reveal eroded scale edges (Fig. 1a). The surface potential appears uniform on the cuticle surface, but clearly increases close to the cuticle edges, suggesting that these regions are more polar. A horizontal section is shown in Fig. 1c and reveals a variation of about 0.7 V between the highest value measured close to the edge of the cuticle and that measured far from the edge. Many different sections have been analyzed on different images and the range of potential variation between the edge and the center of the cuticles is between 0.4 and 0.8 V. To ensure that the measured values were not due to artefacts, we varied the tension applied to the tip. No change was observed on the images and the surface potential differences were found independent of the voltage applied to the tip.

Therefore, we conclude that the edges are more polar than the other exposed parts of the cuticles. These differences can be related to the molecular structure of the cuticles. It is well known that the outer surface of the cuticle cells, the epicuticle, is essentially made of fatty substances (particularly several fatty acids, among them 18-methyleicosanoic acid, stearic acid, palmitic acid, and oleic acid) [21]. On the other hand, the edges are regions where important concentrations of proteins are observed. Surface potential is a measure of the density and orientation of molecular dipole moments (or even possibly ionized protein groups under a water adsorbed layer) and reflects the local polarity of the surface. The differences revealed here by surface potential imaging are likely due essentially to the more polar environment created by proteins.

It must be noted that some debris, which could be attributed to endocuticular debris, is observed on several occasions (Figs. 1 and 5) [6]. Surface potential images reveal that this debris seems to be quite polar as the border of the scales. This could be related to the particular composition of the endocuticle, which is known to be rich in proteins [1].

#### 3.2. Wetting experiments

To correlate the surface potential imaging observations with other properties, wetting experiments were performed on hair samples using different liquids. Two different techniques were used, depending on the nature of the liquid:

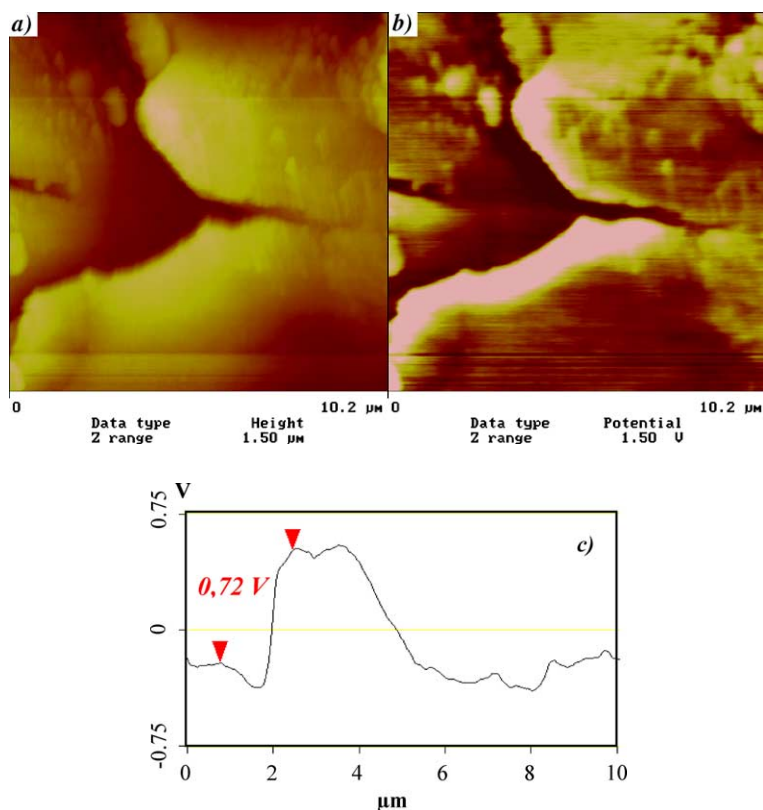


Fig. 1. (a) Tapping mode AFM image of a European black hair. (b) Surface potential image of the same region. (c) Cross section profile showing dimensions of the surface features along the line indicated in the surface potential image. The value in italics indicates the measured surface potential between the two solid triangles.

- For nonvolatile liquids, a deposition technique was used: small drops of liquid were directly deposited on the hair by using a microsyringe. Similar experiments were performed previously on small drops on flat substrates [22,23], but only when a noncontact mode is used can unperturbed droplets be imaged [24]. When the tip is too close to the liquid surface, the liquid is attracted to the tip and instabilities are observed [25], which are very characteristic of these liquid surfaces. The appearance of instabilities is therefore a useful signature of the presence of liquid on the surface. Note that using this technique, a possible local dewetting of the hair may occur, due to the interaction with the deposited liquid on the substrate.
- For volatile liquids, a condensation technique was used: by putting the hair sample on top of a liquid reservoir, we create conditions such that the liquid can condense directly on the hair. One then tests the heterogeneous nucleation at a local scale.

A simple way to predict the wetting properties of a liquid on a surface consists of comparing the solid critical surface tension  $\gamma_c$  with the surface tension of the liquid  $\gamma$  [26]. If  $\gamma > \gamma_c$ , partial wetting occurs with a finite contact angle  $\theta$ . If  $\gamma < \gamma_c$ , a thin layer of liquid spreads the surface (complete wetting,  $\theta = 0$ ). Several liquids with different surface

tensions were used during the experiments and were found to exhibit various behaviors (Table 1). The results obtained for the different liquids are as follows.

### 3.2.1. Water

The experiments were performed using a droplet of water in contact with the hair glued on a silicon wafer. The water quickly evaporates from the surface of the substrate, and no evidence of wetting on the hair surface is observed: the images are similar to those of a dry hair and no instabilities are observed. Moreover, the diameter of the hair sample increased with time as clearly indicated by a slow drift in the Z position of the scanner during the scans. The hair is indeed porous and can take up a large amount of water (typically up to 35% of its own weight).

### 3.2.2. Glycerol

Glycerol is a polar liquid which is much less volatile than water under standard conditions and is known not to penetrate the hair, as checked by the absence of shift of the scanner during AFM measurements. However, results similar to those for water were obtained: no instabilities were detected, indicating that the cuticle remained dry.

### 3.2.3. Squalane

Squalane is also expected neither to penetrate, nor to evaporate, on the experimental timescale. Its behavior is very

Table 1

	Silicone oil (PDMS)	Decane <sup>a</sup>	Dodecane	Squalane	Glycerol	Water
Surface tension $\gamma$ (mN/m)	21	23.4	25.6	31.1	64	72.8
Wetting behavior	Liquid layer on the hair (total wetting)	Liquid seen along the borders of the cuticle cells Sometimes liquid covers a part of the cuticular surface		Liquid seen along the borders of the cuticle cells	No liquid found on the surface (no wetting)	

<sup>a</sup> Indirect wetting method.

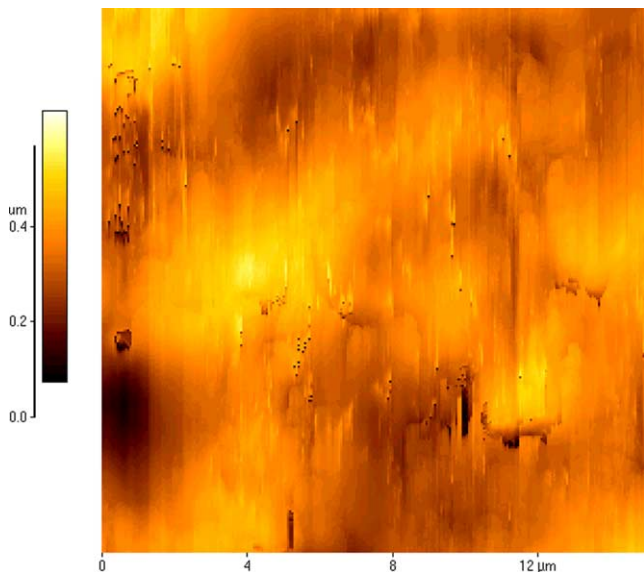
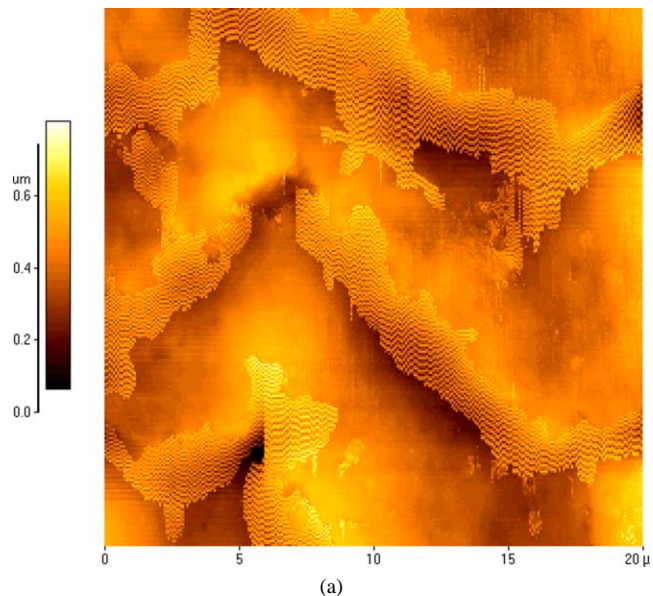


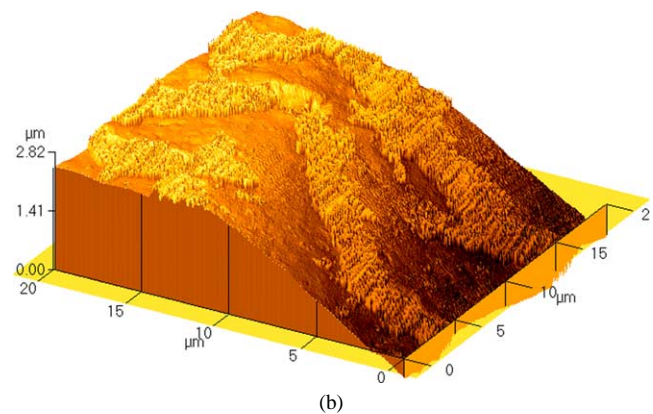
Fig. 2. Topographic image of a hair sample wetted by squalane. The image was taken immediately after liquid deposition.

different from that of water and glycerol: immediately after the deposition of a small droplet on the top of the hair using a microsyringe (typical volume around 1  $\mu\text{l}$ ), a smoothing of the cuticles features is detected, as if the surface topography was hidden by a squalane layer (Fig. 2).

To ensure that these observations were not due to contamination of the tip by the liquid, experiments were performed with the same tip but with a new dry hair (without squalane), keeping the same imaging parameters. The topographic images confirmed that the tip was free of contamination: the sharp details of the cuticles were recovered. When new images of the sample covered by squalane were taken with the same tip, smoothed features such as those of Fig. 2 were recovered. We then conclude that a layer of squalane remains on the sample. A small droplet of squalane, about 1  $\mu\text{l}$ , seems to be sufficient to cover several centimeters of hair. After a period of 2 h, drainage removes squalane from the top of the hair and it turns out that instabilities appear along the borders of the scales (Fig. 3). These instabilities reveal the presence of liquid, indicating that squalane prefers to accumulate on the edges. The nature of these instabilities has been studied



(a)



(b)

Fig. 3. Topographic image of a hair sample wetted by squalane (a) and associated 3-dimensional perspective (b). The image was taken 2 h after liquid deposition.

in detail by Dubreuil et al. [25]. The top of the cuticle can be accurately imaged, without any evidence of being wet.

### 3.2.4. Decane and dodecane

Two other alkanes were investigated, decane and dodecane, which are more volatile than squalane. It then becomes delicate to observe the wetting properties using the direct



Fig. 4. Optical image of hair sample wetted by decane using the condensation method. A liquid film is seen on the sides of the hair, as well as on the wafer.

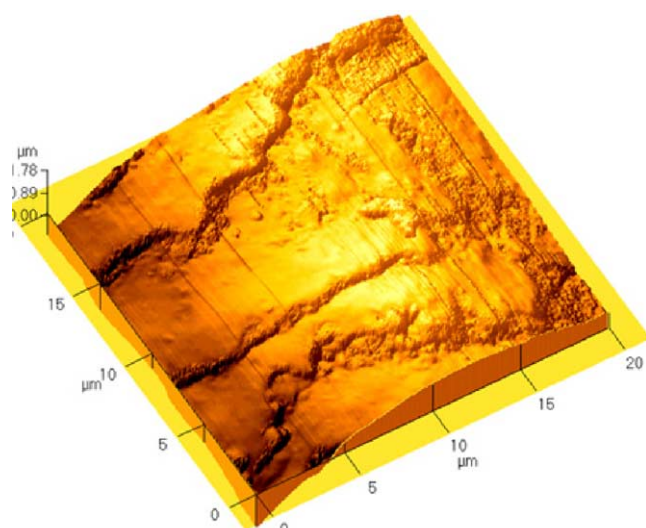


Fig. 5. Topographic image of hair wetted by decane, taken 4 h after exposure to decane vapor. Note that instabilities are mainly present along the cuticle edges, which indicates that decane prefers to accumulate along these edges. The top of the cuticles is still relatively smooth, and does not show evidence of being wet.

wetting method described above. In order to avoid drawbacks due to decane or dodecane evaporation, we created conditions such that the liquid could condense directly on the hair. This hair was cut and fixed onto a silicon wafer, placed into a specially designed cell containing the AFM probe and the sample [24]. The cell can be saturated with alkane vapor until many drops are seen to condense on the wafer (Fig. 4). When the surface of the hair was imaged, droplets were never observed on the top of the hair, suggesting that the liquid was able either to penetrate or to fully spread onto the hair surface. Images were captured over a period of several hours. During approximately 3 h, the wafer was clearly wet by droplets, but no liquid drop appears on the hair surface. After three hours, typical liquid instabilities could be observed along the edge of the cuticles (Fig. 5). The presence of endocuticular debris could explain why instabilities are sometimes noticed on the flat part of the cuticle surface: the endocuticle is known to be richer in protein and thus less hydrophobic than the outermost layer, the epicuticle, essentially made of lipids [1]. However, no drop-like condensation

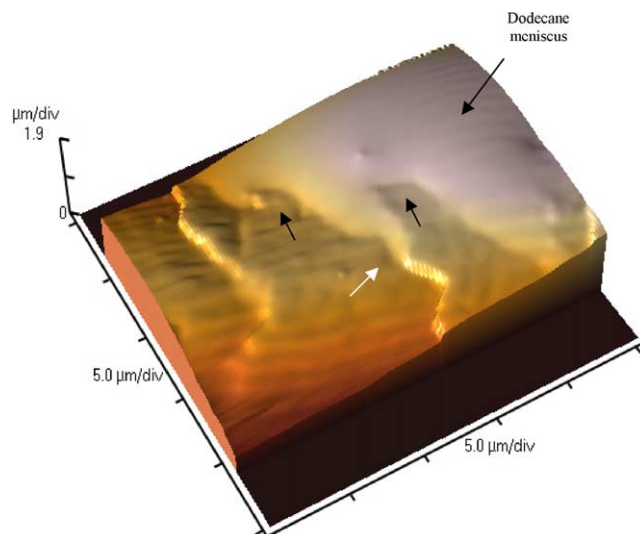


Fig. 6. NC-AFM image showing the edge of a dodecane drop wetting several hair cuticle cells. The liquid partially wets the top of cuticle cells (black arrows) with a local contact angle of approximately  $12^\circ$ . Conversely it spreads more along the more wettable cell edges (white arrow). Note that the longitudinal striations are likely due to an artefact.

was observed on the hair surface. This observation is discussed below in terms of competitive penetration, nucleation and/or dewetting.

However, droplets wetting the hair are expected to have a distorted contact line due to the chemical and geometrical (roughness) heterogeneities of the surface. This can be clearly seen in Fig. 6, showing a large dodecane droplet wetting several cuticles. Notice that liquid spreads more along the more wettable edge of the cuticle. The same features could also be observed with decane by using the condensation method, although less neatly. On Fig. 6, longitudinal striations could be seen. Such striations are likely due to an artefact that appears during the scanning by the tip (probably remaining optical interferences) since they are also observed on the liquid part. These striations are thus certainly different from the ones observed by Swift and colleagues on different mammalian fibers, which present a typical spacing always in the range from 0.3 to 0.4  $\mu\text{m}$  [27,28].

### 3.2.5. Silicone oil

Using silicone oil, a liquid of smaller surface tension (PDMS, viscosity of 100 cS), a liquid layer on the hair was observed in all experiments, and the details of the cuticle surface were blurred as in the squalane case. We conclude that silicone oil spreads very quickly on the hair and the substrate surface. Such behavior is in agreement with observations made by Cazabat et al., who reported that silicone oil spreads on all surfaces regardless of their nature (hydrophilic or hydrophobic) [29].

The findings obtained for the different liquids used are summarized in Table 1.

#### 4. Discussion

It is well known that hair surfaces are covered by a compact hydrophobic layer, the epicuticle, mainly made of close-packed fatty acid chains [1,21]. Nevertheless, hair surfaces are not chemically homogeneous: though the surface composition is not yet accurately known, one can assume that the surface chemical moieties of the flat part of the outer hair cells (scales) consist of methyl and methylene groups. For such a surface, one could reasonably expect a critical surface tension  $\gamma_c$  between 22 and 31 mN/m, respectively the values found for pure methyl-like and pure methylene-like surfaces [30,31]. On the other hand, the side of the cells is covered in part by proteins, for which a higher value of the critical surface tension is expected.

Let us discuss the results obtained according to the notion of critical surface tension and consider separately the cases of the flat part and of the sides of the outer hair cells:

If the outer hair cell surfaces are predominantly covered by compact methyl groups,  $\gamma_c$  must be about 22 mN/m. When  $\gamma > \gamma_c$ , partial wetting of the liquid should be observed with a measurable contact angle. Most liquids used in these experiments have a surface tension higher than 22 mN/m, implying a partial wetting on the outer surface of the scales (Table 1). Whereas the observations made with these liquids did not show any spreading, no drops were observed either. Nevertheless, such results are not contradictory when one considers the particular behavior of the liquids. With water, a swelling of the hair fiber is observed, indicating that the liquid penetrates the fiber. Water can also evaporate fast, being quite volatile. Glycerol is known not to penetrate the hair and it probably quickly dewets the outer surface of the scales. These assumptions also explain why no evidence of wetting was observed on the borders of the scales in spite of the higher value of the expected surface tension.

Squalane is known neither to penetrate nor to evaporate on the experimental timescale. The observations made by using this liquid show that it dewets less quickly than glycerol: immediately after the deposition, a layer of squalane covers the sample. After several hours, drainage removes squalane from the top of the hair and instabilities appear on the borders, indicating that squalane prefers to accumulate on the edges (some of it is left wetting the edges). This observation is in agreement with a complete wetting on the borders ( $\gamma < \gamma_c$ ). Decane and dodecane are more volatile than squalane and are suspected of penetrating the hair. These two liquids may nucleate drops which are not seen because they quickly penetrate the hair. For these alkanes, the difference between  $\gamma$  and  $\gamma_c$  is very small and this could explain why some images reveal that these liquids sometimes cover a part of the scales (Figs. 5 and 6). More likely, nucleation of drops mainly occurs on the edges where a higher critical surface tension is expected. Silicone oil is the only liquid with a surface tension lower than 22 mN/m. In this case, a ho-

mogeneous liquid layer covers the entire surface of the hair, which is consistent with a complete spreading when  $\gamma < \gamma_c$ .

If the outer hair cell surfaces were predominantly covered by compact methylene groups, a higher value of  $\gamma_c$  is expected, about 31 mN/m. Most conclusions which have been put forward for the different liquids under the hypothesis of  $\gamma_c = 22$  mN/m are still valid: water penetrates into the bulk of the hair fiber, glycerol probably dewets quickly and/or is pumped out by glycerol on the solid substrate and squalane dewets less quickly and some of it is left wetting the edges. With decane and dodecane,  $\gamma_c$  is then lower than  $\gamma$ , implying a complete spreading. These two liquids may nucleate everywhere but still more preferentially on the border of the scales where a thicker film may pump out the film nucleated on the scale. Taking into account a likely penetration of the liquid may explain why no evidence of the presence of these liquids was found on the flat part of the outer hair scales. In the case of silicone oil, complete spreading is expected ( $\gamma < \gamma_c$ ), which is in agreement with the observed behavior.

To summarize, the value of the critical surface tension for the flat part of the cells is probably between 22 and 31 mN/m. It cannot be estimated with more precision at this time, because of the possibility of penetration of the two liquids used with tensions intermediate between these two values (decane and dodecane). Nevertheless, the results are in agreement with a critical surface tension due to a mixing of methyl and methylene-like surface groups. The critical surface tension of the cell borders is certainly larger.

#### 5. Conclusions

In this paper we have reported investigations of wetting and electrostatic properties of hair by atomic force microscopy. Surface potential imaging was used to characterize local polarities, while wetting properties were investigated by imaging hair samples on which different liquids were spread, by using noncontact mode AFM. We found a remarkable concordance between the surface potential experiments, reflecting the cartography of the polarity of the hair surface, and the location of hydrocarbon liquids during the wetting process of this hair: these liquids preferentially wet the cuticles edges which are more polar. More polar liquids such as water and glycerol do not appear to wet any region of the cuticle, although water was seen to penetrate into the bulk of the hair fiber.

#### References

- [1] M. Feughelman, Mechanical Properties and Structure of Alpha-Keratin Fibers: Wool, Human Hair and Related Fibres, University of New South Wales Press, 1997.
- [2] M.S.C. Birbeck, E. Mercer, J. Biophys. Biochem. Cytol. 3 (1957) 223–233.
- [3] J.A. Swift, A.W. Holmes, Textile Res. J. 35 (1965) 1014.
- [4] L. Wolfram, M. Lindermann, J. Soc. Cosmet. Chem. 22 (1971) 839–850.

- [5] J.A. Swift, B.W. Bews, *J. Soc. Cosmet. Chem.* 25 (1974) 13–33.
- [6] J.A. Swift, *Int. J. Cosmet. Sci.* 13 (1991) 143–159.
- [7] L. Kreplak, C. Mériçoux, F. Briki, D. Flot, J. Doucet, *Biochim. Biophys. Acta* 1547 (2001) 268–274.
- [8] S.D. O'Connor, K.L. Komisarek, J.D. Baldeschwielder, *J. Invest. Dermatol.* 105 (1995) 96–99.
- [9] H. You, L. Yu, *Scanning* 19 (1997) 431–437.
- [10] J.R. Smith, *J. Soc. Cosmet. Chem.* 48 (1997) 199–208.
- [11] R.L. McMullen, et al., *IFSCC Mag.* 3 (3) (2000) 39–44.
- [12] J.A. Swift, J.R. Smith, *Scanning* 22 (2000) 310–318.
- [13] F.J. Carrion-Fite, *Textile Res. J.* 64 (1) (1994) 49–55.
- [14] Y. Gu, D. Li, P. Cheng, *Colloids Surf. A* 122 (1997) 135–149.
- [15] R. Molina, F. Comelles, M.R. Julià, P. Erra, *J. Colloid Interface Sci.* 237 (2001) 40–46.
- [16] A. Perwuelz, T.N. DeOlivera, C. Caze, *Colloids Surf. A* 147 (1999) 317.
- [17] D. Quéré, J.M. di Meglio, F. Brochard, *Science* 249 (1990) 1256.
- [18] H. Alter, H. Cook, *J. Colloid Interface Sci.* 29 (3) (1969) 439–443.
- [19] H.O. Jacobs, H.F. Knapp, S. Müller, A. Stemmer, *Ultramicroscopy* 69 (1997) 39.
- [20] H.O. Jacobs, H.F. Knapp, A. Stemmer, *Rev. Sci. Instrum.* 70 (3) (1999) 1756–1760.
- [21] A.P. Negri, H.J. Cornell, D.E. Rivett, *Textile Res. J.* 63 (1993) 109.
- [22] F. Rieutord, M. Salmeron, *J. Phys. Chem.* 102 (1998) 3941.
- [23] S. Hermingaus, A. Fery, D. Reim, *Ultramicroscopy* 69 (1997) 211.
- [24] A. Checco, J. Daillant, P. Guenoun, *Phys. Rev. Letts.*, in press.
- [25] F. Dubreuil, P. Guenoun, J. Daillant, *Langmuir*, in press.
- [26] W.A. Zisman, *Adv. Chem. Ser.* 43 (1964) 1.
- [27] J.A. Swift, J.R. Smith, in: *Proceedings of the 10th Internat. Wool Textile Res. Conference, HH-1, 2000*, pp. 1–9.
- [28] J.A. Swift, J.R. Smith, *J. Microsc.* 204 (2001) 203–211.
- [29] A.M. Cazabat, S. Gerdes, M.P. Valignat, S. Vilette, *Interface Sci.* 5 (1997) 129.
- [30] A.W. Adamson, *Physical Chemistry of Surfaces*, Wiley–Interscience, New York, 1990.
- [31] E.G. Shafrin, W.A. Zisman, *J. Phys. Chem.* 64 (1960) 519.